Hindawi Publishing Corporation
EURASIP Journal on Wireless Communications and Networking
Volume 2010, Article ID 945427, 10 pages
doi:10.1155/2010/945427

Research Article

An Efficient Measure for Nonlinear Distortion Severity due to HPA in Downlink DS-CDMA Signals

Tarek K. Helaly, Richard M. Dansereau, and Mohamed El-Tanany

Department of Systems and Computer Engineering, Carleton University, 1125 Colonel By Drive, Ottawa, ON, Canada K1S 5B6

Correspondence should be addressed to Tarek K. Helaly, thelaly@sce.carleton.ca

Received 22 June 2010; Revised 8 September 2010; Accepted 4 October 2010

Academic Editor: Fabrizio Granelli

This paper deals with the nonlinear distortion (NLD) effects of high power amplifiers (HPAs) on direct sequence-code division multiple access systems. Such a distortion drastically degrades the system performance in terms of bit error rate (BER) degradation and spectral regrowth. Much effort has been conducted to minimize NLD. A key requirement to do so is to define a certain measure for the HPA nonlinearity, which when reduced often allows NLD to also be reduced. Several measures were proposed such as peak-to-average power ratio, instantaneous power variance, and cubic metric. In this paper, we show that such measures are not closely related to NLD and their reduction does not always lead to optimum performance. Hence, we introduce an efficient measure, namely, nonlinearity severity (NLS), to characterize NLD effects, as an alternative to the existing measures. The NLS is characterized by having direct link to the system performance as it is formulated based on the signal characteristics contributing to BER performance and spectral regrowth. Additionally, a major advantage of the NLS measure is that it is linked to the IBO level allowing the possibility of improving performance at all IBO levels of interest.

1. Introduction

Downlink direct sequence-code division multiple access (DS-CDMA) signals typically exhibit large dynamic range. This large dynamic range results in signal distortion for components falling in the highly nonlinear regions of the high power amplifier (HPA) characteristics. This nonlinear distortion (NLD) degrades the bit error rate (BER) and creates out-of-band emissions in adjacent channels known as spectral regrowth.

Over the decades, much research has been conducted to reduce the vulnerability of the amplifier input signal to nonlinearity. Such research often seeks to define a measure for NLD, which when reduced often allows NLD to also be reduced. Several measures were adopted to quantify NLD in relation to the input signal to the HPA such as peak-to-average power ratio (PAR) [1, 2], the instantaneous power variance (IPV) [3, 4], and the cubic metric (CM) [5, 6].

Reduction of such measures does achieve remarkable performance improvements that, in turn, enhance the system performance or the HPA efficiency. While the existing measures have their use, it is not mathematically clear how they relate to the system performance in terms of BER or spectral regrowth. Moreover, no close relation between these measures and IBO level of interest exists, which is important in determining the IBO required to work at according to design demands or service regulations. Consequently, reduction of such measures does not always lead to optimum performance as will be demonstrated later.

In [7, 8], we explored which signal characteristics at a predistorter-HPA's (PD-HPA) input are responsible for performance degradation (BER degradation and spectral regrowth). Based on such characteristics, in this paper, we introduce an efficient measure for characterizing NLD, namely, nonlinearity severity (NLS) measure, as an alternative to the existing measures, which is characterized by having a direct link to the system performance.

This paper is organized as follows. In Section 2, the DS-CDMA system under investigation is described. In Section 3, the signal characteristics established in [7, 8] that contribute to the BER degradation and spectral regrowth are presented, in order to provide the reader with the theory upon which the proposed measure is based. In Section 4, we present a brief survey on the most currently known nonlinearity measures highlighting their advantages and disadvantages. In Section 5, the proposed NLS measure is developed. In Section 6, the performance of the NLS measure is assessed in comparison with PAR. Finally, Section 7 summarizes the conclusions drawn from the paper.

2. Existing Nonlinearity Measures

The system under investigation is a downlink synchronous DS-CDMA system, where users' signals have equal power. The complex envelope of the nth DS-CDMA symbol for K active users is defined as [7]

$$\begin{aligned} s(t) &= \sum_{k=1}^{K} \sqrt{E_s} a_n^{(k)} c^{(k)}(t) \\ &= r(t) e^{j\theta(t)}, \quad (n-1)T \le t \le nT, \end{aligned} \tag{1}$$

where E_s is the kth user's signal energy per symbol, T is the symbol duration, $a_n^{(k)}$ are the kth user's symbol data, $r(t) = |s(t)|$, $\theta(t) = \angle\, s(t)$, and

$$c^{(k)}(t) = \sum_{l=0}^{L-1} c_l^{(k)} h(t - lT_c) \tag{2}$$

is the spreading waveform obtained with the Walsh-Hadamard matrix, L is the spreading factor, $T_c = T/L$ is the chip duration, and $h(t)$ is the impulse response of the pulse shaping filter. Without loss of generality, the spreading waveforms are assumed to have unit energy, that is, $\int_0^T [c^{(k)}(t)]^2 dt = 1$.

A PD-HPA pair is considered as the nonlinear amplifier chain, which has a zero AM-PM characteristic $\Phi[r(t)]$ and an AM-AM characteristic given by

$$r_d(t) = G[r(t)] = \begin{cases} r(t) & 0 \le r(t) \le \zeta, \\ \zeta & r(t) > \zeta, \end{cases} \tag{3}$$

where ζ is the saturation (clipping) threshold. In practice, the input/output characteristics of the PD-HPA are slightly different due to misalignment between the predistorter and HPA. However, such a slight difference will not greatly affect the performance, and, hence, the assumed ideal PD-HPA sufficiently serves the analysis approach. Finally, the output from the PD-HPA can be expressed as [7]

$$\begin{aligned} s_d(t) &= r_d(t) e^{j(\theta(t) + \Phi[r(t)])} \\ &= (r(t) - r_c(t)) e^{j\theta(t)} = s(t) - s_c(t), \end{aligned} \tag{4}$$

where $s_c(t) = r_c(t)e^{j\theta(t)}$ is the clipped portion of the input signal $s(t)$, $E\{s_c(t)\} = 0$, and its envelope $r_c(t)$ has the form

$$r_c(t) = r(t) - r_d(t) = \begin{cases} 0 & r(t) \le \zeta, \\ r(t) - \zeta & r(t) > \zeta. \end{cases} \tag{5}$$

3. Signal Characteristics Contributing NLD Effects

In this section, we shed light on the signal characteristics that contribute to the BER degradation and spectral regrowth presented in [7] and [8], respectively. The purpose of this section is to make sure the reader is familiar with the theoretical background, which we will rely upon for the formulation of the proposed measure NLS.

3.1. BER Degradation. Consider the CDMA signal in (1), where the symbols $a_n^{(k)}$ are assumed equiprobable i.i.d. with zero mean and variance of $E\{|a_n^{(k)}|^2\}$, and belong to alphabet $\mathcal{A}$ of size M with $\mathcal{A} \in \{\pm 1/\sqrt{2} \pm j1/\sqrt{2}\}$.

For large number of users and assuming the pulse shaping filter corresponds to a square root raised cosine (SRRC) filter with small roll-off factor, $s(t)$ can be regarded as a band-limited zero-mean complex Gaussian process with variance $\sigma_s^2 = E_s \sum_{k=1}^{K} E\{|a_n^{(k)}|^2\} = KE_s$ and an envelope $r(t)$ having a quasi-Rayleigh pdf $f_r(r) = (2r/\sigma_s^2)e^{-r^2/\sigma_s^2}$, $r \ge 0$ [9].

It is more convenient in the context of this paper to use the IBO level instead of the threshold ζ, where the IBO, γ, is defined as the ratio of the input power at the saturation level P_{sat} to the signal average power P_{av}. That is, $\gamma = \zeta^2/\sigma_s^2$.

The output of the PD-HPA can be represented as the sum of two uncorrelated components: a scaled linear component and a nonlinear component, $n(t)$ [9–11], that is,

$$s_d(t) = \alpha_0 s(t) + n(t), \tag{6}$$

where $E\{n(t)\} = 0$, $E\{s(t)n^*(t+\tau)\} = 0$, for all t, τ, and α_0 is the linear gain given by

$$\begin{aligned} \alpha_0 &= \frac{E\left\{s_d^*(t)s(t)\right\}}{E\left\{|s(t)|^2\right\}} = \frac{E\{r_d(t)r(t)\}}{E\{r^2(t)\}} \\ &= \frac{1}{2\sigma_x^2}\left(\int_0^{\zeta} r^2 f_r(r)dr + \zeta \int_{\zeta}^{\infty} r f_r(r)dr\right) \\ &= 1 - e^{-\gamma} + \frac{1}{2}\sqrt{\pi\gamma}\ \text{erfc}\left(\sqrt{\gamma}\right). \end{aligned} \tag{7}$$

The variance of the distorted signal $s_d(t)$ is given by $\sigma_d^2 = |\alpha_0|^2 \sigma_s^2 + \sigma_n^2$, where σ_n^2 is the variance of the nonlinear component $n(t)$. As far as $s(t)$ is considered as a zero-mean Gaussian process, σ_d^2 can be calculated as

$$\begin{aligned} \sigma_d^2 &= E\left\{|s_d(t)|^2\right\} = \int_0^{\zeta} r^2 f_r(r)dr + \int_{\zeta}^{\infty} \zeta^2 f_r(r)dr \\ &= \sigma_s^2\left(1 - e^{-\zeta^2/\sigma_s^2}\right) = \sigma_s^2(1 - e^{-\gamma}). \end{aligned} \tag{8}$$

At the kth user's receiver, complex zero-mean additive white Gaussian noise (AWGN) $w(t)$ with power spectral density of $N_0/2$ is introduced, and the received signal is expressed as $u(t) = s_d(t) + w(t) = \alpha_0 s(t) + n(t) + w(t)$. Assuming perfect synchronization, after coherent demodulation and phase recovery, the received signal is match-filtered with

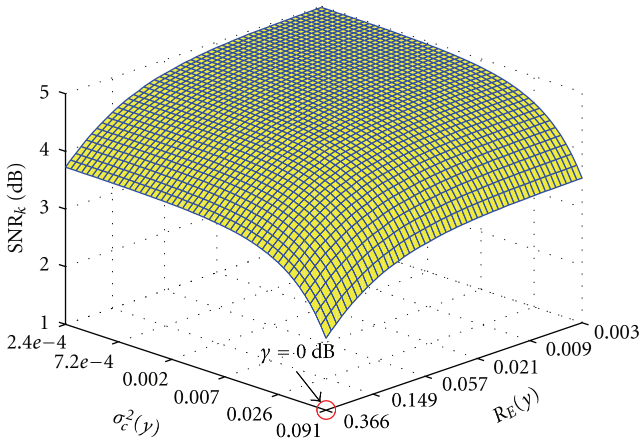

Figure 1: SNR_k versus R_E and σ_c^2 at $\text{SNR}_{\text{AWGN},k} = 5$ dB.

the kth user's spreading waveform $c^{(k)}(t)$ and passed to the detector. Thus, the signal-to-noise ratio (SNR) per bit at the kth detector input is given by

$$\text{SNR}_k = \frac{|\alpha_0|^2 \sigma_{s,k}^2 / \log_2 M}{\sigma_W^2 + |\alpha_0|^2 \sigma_S^2 / \log_2 M + \sigma_N^2 / \log_2 M}, \qquad (9)$$

where $\sigma_{s,k}^2 = \sigma_s^2/K$ is the kth user power, $\sigma_W^2 = (N_0/2)\int_0^T [c^{(k)}(t)]^2 dt = N_0/2$ is the variance of the AWGN component [12, equation (15.329)], σ_N^2 is the variance of the nonlinear component $n(t)$, and σ_S^2 is the variance of the interference from the other users. For sufficiently large K and L, σ_S^2 and σ_N^2 can be assumed Gaussian distributed given by $\sigma_N^2 = (1/L)E\{|n(t)|^2\}\int_0^T [c^{(k)}(t)]^2 dt = (\sigma_n^2/L) = (\sigma_d^2 - |\alpha_0|^2\sigma_s^2)/L$ and $\sigma_S^2 = \sigma_s^2(K-1)/KL$ (for synchronous CDMA and equal users' powers), respectively (see [10] and the references therein). Since we are considering the Walsh orthogonal codes, σ_S^2 vanishes. The issue of the other user interference was handled in [7] using a decorrelating detector, where it is eliminated at the expense of noise enhancement.

Therefore, SNR_k in (9) will be

$$\text{SNR}_k = \frac{|\alpha_0|^2}{\text{SNR}_{\text{AWGN},k}^{-1} + \left(1/L\sigma_{s,k}^2\right)\left(\sigma_d^2 - |\alpha_0|^2\sigma_s^2\right)}, \qquad (10)$$

where $\text{SNR}_{\text{AWGN},k} = (\sigma_{s,k}^2/\log_2 M)/\sigma_W^2$ is the SNR per bit at the kth detector due to the AWGN only (without nonlinearity).

Let us define two important characteristics of the input signal in relation to the PD-HPA. First, the threshold exceeding rate R_E is defined as the total time intervals where the signal exceeds the PD-HPA threshold or equivalently the probability that the signal exceeds the threshold ζ

$$R_E = P(r > \zeta) = \int_\zeta^\infty f_r(r)dr = e^{-\zeta^2/2\sigma_x^2} = e^{-\gamma}. \qquad (11)$$

Second, the variance of the clipped signal portion $s_c(t)$, σ_c^2, is given as

$$\begin{aligned}\sigma_c^2 &= E\left\{|s_c(t)|^2\right\} = \int_\zeta^\infty (r-\zeta)^2 f_r(r)dr \\ &= \sigma_s^2\left(e^{-\gamma} - \sqrt{\pi\gamma}\,\text{erfc}\left(\sqrt{\gamma}\right)\right).\end{aligned} \qquad (12)$$

Rearranging (11) and (12) and substituting in (7) and (8), respectively, give

$$\alpha_0 = 1 - \frac{R_E}{2} - \frac{\sigma_c^2}{2\sigma_s^2}, \qquad (13)$$

$$\sigma_d^2 = \sigma_s^2(1 - R_E). \qquad (14)$$

Substituting (13) and (14) in (10), we obtain

$$\text{SNR}_k = \frac{1}{4}\frac{\left(2 - R_E - \sigma_c^2/\sigma_s^2\right)^2}{\text{SNR}_{\text{AWGN},k}^{-1} + (K/L)\left(\sigma_c^2/\sigma_s^2 - (1/4)\left(R_E + \sigma_c^2/\sigma_s^2\right)^2\right)}. \qquad (15)$$

It is concluded from (15) that the signal characteristics R_E and σ_c^2 represent the main contributors to NLD effects. In order to visualize the impact of such characteristics on the system performance, the SNR in (15) is computed at $\text{SNR}_{\text{AWGN},k}$ of 5 dB and plotted against R_E and σ_c^2 in Figure 1. Computations are done at different IBO levels ranging from 0 dB up to the level that passes almost all of the signal without clipping, that is, $R_E \cong \sigma_c^2 \cong 0$. Finally, the BER performance for the considered QPSK modulation is given by

$$\text{BER}_k = Q\left(\sqrt{\frac{(1/4)\left(2 - R_E - \sigma_c^2/\sigma_s^2\right)^2}{\text{SNR}_{\text{AWGN},k}^{-1} + (K/L)\left(\sigma_c^2/\sigma_s^2 - (1/4)\left(R_E + \sigma_c^2/\sigma_s^2\right)^2\right)}}\right). \qquad (16)$$

The importance of such a BER expression is that it is formulated based on the signal characteristics in relation to the PD-HPA characteristics. This new characterization opens new avenues to minimize NLD via controlling such characteristics as will be demonstrated later; as R_E and σ_c^2 increase, the overall SNR decreases. In order to visualize the impact of the CDMA signal characteristics R_E and σ_c^2 on the system performance, the SNR in (15) is computed at $\text{SNR}_{\text{AWGN},k}$ of 5 dB and plotted against R_E and σ_c^2 in Figure 1. Computations are done at different IBO levels ranging from 0 dB up to the level that passes almost all of the signal without clipping, that is, $R_E \cong \sigma_c^2 \cong 0$.

3.2. Spectral Regrowth. Since the modulated CDMA signal in (1) is cyclostationary, the PD-HPA output signal $s_d(t)$ in (4) is also cyclostationary. Cyclostationarity is a special case of stationary, which describes a probabilistic model for certain random data that involves certain periodicity model.

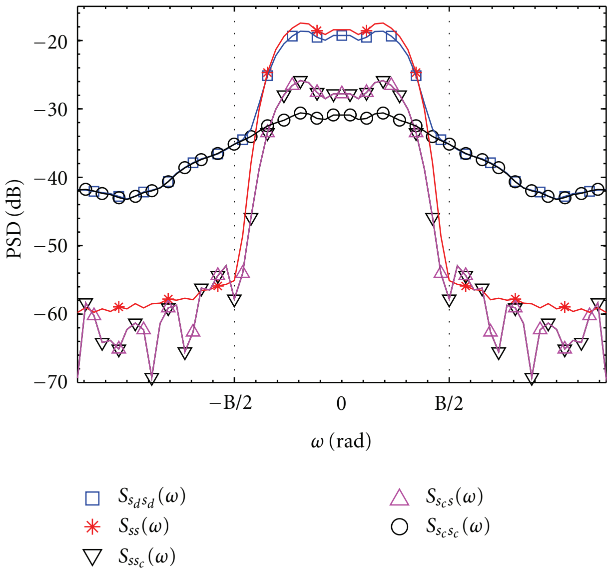

Figure 2: PSDs in (19) for an SRRC-filtered, 16-user baseband CDMA signal.

For instance, a cyclostationary signal $s(t)$ has a periodic autocorrelation function, that is, $R_{ss}(\tau) = R_{ss}(\tau + T)$. Such a periodicity advantage is not of a major importance for the purpose of analysis of this paper. Therefore, we use the ordinary autocorrelation function of stationary random signals for $s_d(t)$, which is given by

$$\begin{aligned} R_{s_d s_d}(\tau) &= E\{s_d(t)s_d(t+\tau)\} \\ &= R_{ss}(\tau) - R_{ss_c}(\tau) - R_{s_c s}(\tau) + R_{s_c s_c}(\tau), \end{aligned} \tag{17}$$

where $R_{ij}(\tau)$ represents the cross-correlation function of the arbitrary signals $i(t)$ and $j(t)$. The Fourier transform of the autocorrelation function gives the PSD of the output signal as

$$S_{s_d s_d}(\omega) = S_{ss}(\omega) - S_{ss_c}(\omega) - S_{s_c s}(\omega) + S_{s_c s_c}(\omega), \tag{18}$$

where $S_{ss}(\omega)$ is the PSD of the input signal to the PD-HPA, $S_{ss_c}(\omega)$ and $S_{s_c s}(\omega)$ are the cross PSDs of the input signal and the clipped signal portion, and $S_{s_c s_c}(\omega)$ is the PSD of the clipped signal portion.

Figure 2 shows the PSDs in (18) for a 16-user baseband CDMA signal of 100 symbols duration with an SRRC filter with roll-off of 0.22. The PSDs are evaluated using the Welch estimation method with the following parameters: Hamming window and 50% overlap between segments. In order to have an adequate trade-off between estimate reliability and frequency resolution, the segment length is set to 32.

Without loss of generality, spectral regrowth can be defined for the upper channel as the additional out-of-band power at the output of the HPA, that is, $P_{\mathrm{SR}} = \int_{B/2}^{\infty} S_{s_d s_d}(\omega) - S_{ss}(\omega) d\omega$. As shown in Figure 2, the PSD of the clipped signal portion almost coincides with the output distorted PSD outside the signal bandwidth, that is, $S_{s_d s_d}(\omega) \cong S_{s_c s_c}(\omega)$, $|\omega| > B/2$. Also, since the PSD of the baseband filtered CDMA signal is almost rectangular, it can be assumed constant over the entire bandwidth B and zero elsewhere, that is, $S_{ss}(\omega) = 0$, $|\omega| > B/2$. Therefore, $P_{\mathrm{SR}} \cong \int_{B/2}^{\infty} S_{s_c s_c}(\omega) d\omega$, that is, spectral regrowth depends primarily on the PSD of the clipped signal portion, and, in turn, as the variance of the clipped signal portion $\sigma_c^2 = \int_{-\infty}^{\infty} S_{s_c s_c}(\omega) d\omega$ increases, spectral regrowth increases.

Then, a piecewise analysis approach for $s_c(t)$ is adopted to determine what other signal characteristics at the PD-HPA input, in addition to σ_c^2, would contribute to spectral regrowth. In such an approach, $s_c(t)$ can be represented as a piecewise signal, where each piecewise segment $s_{c,i}(t)$ is realized in the interval $[t_{i-1}, t_i)$ with $i = 1, \ldots, I$ to accommodate I segments. Clearly, the I segments alternate between zero for the unclipped regions and $s_c(t)$ for the clipped regions. Without loss of generality, it can be assumed that even values of i correspond to time intervals with clipping and odd values of i correspond to time intervals with no clipping (i.e., $s_c(t) = 0$). Following this convention and with t_0 arbitrarily assigned as $t_0 = 0$ sec, $s_c(t)$ can be represented as

$$\begin{aligned} s_c(t) &= \sum_{\substack{i=1 \\ \text{even}}}^{I} s_{c,i}(t) \\ &= \sum_{\substack{i=1 \\ \text{even}}}^{I} s(t)\left| w_{\mathrm{rect},i}(t;\tau_i) \right| - \zeta w_{\mathrm{rect},i}(t;\tau_i), \end{aligned} \tag{19}$$

where $w_{\mathrm{rect},i}(t;\tau_i)$ are represented by rectangular windows as

$$w_{\mathrm{rect},i}(t;\tau_i) = \begin{cases} \operatorname{sgn}\{s(t)\}, & t_i - \tau_i \le t < t_i, \\ 0, & \text{otherwise}, \end{cases} \tag{20}$$

where $\operatorname{sgn}\{s(t)\} = s(t)/|s(t)|$ and $\tau_i = t_i - t_{i-1}$ is the duration of the ith piecewise segment.

Using the definition of $s(t)$ in (1), $s_c(t)$ can be written as

$$\begin{aligned} s_c(t) = \sum_{\substack{i=1 \\ i\ \text{even}}}^{I} \Bigg[& \sum_{k=1}^{K} \sqrt{E_s} a_n^{(k)} \sum_{l=0}^{L-1} c_l^{(k)} h(t - lT_c) \left| w_{\mathrm{rect},i}(t;\tau_i) \right| \\ & - \zeta\, w_{\mathrm{rect},i}(t;\tau_i) \Bigg]. \end{aligned} \tag{21}$$

Taking the Fourier transform of (21), $S_c(\omega) = \mathcal{F}\{s(t)\}$, the power spectrum of the clipped signal portion can be written as

$$S_{s_c s_c}(\omega) = |S_c(\omega)|^2 = \left| \sum_{\substack{i=1 \\ i \text{ even}}}^{I} \left[\sum_{k=1}^{K} \sqrt{E_k} a_n^{(k)} \sum_{l=0}^{L-1} c_l^{(k)} e^{-j\omega l T_c} G_i(\omega) - \zeta W_{\text{rect},i}(\omega) \right] \right|^2, \tag{22}$$

where

$$G_i(\omega) = H(\omega) * |W_{\text{rect},i}(\omega)|, \tag{23}$$

where $*$ is the convolution operator.

In the frequency domain, the rectangular windows $w_{\text{rect},\,i}(t;\tau_i)$, $i = 1,\ldots,I$, form a set of sinc functions with main lobe widths that are inversely proportional to the durations τ_i's of the clipped subintervals in the time domain. At each new clipping event i, the sinc function $W_{\text{rect},i}(\omega)$, when convolved with the frequency response of the pulse shaping filter $H(\omega)$ with arbitrary bandwidth B as in (23), results in $G_i(\omega)$ with bandwidth $B_i > B$. Consequently, given the power spectrum of the clipped signal portion in (22), it is concluded that as the number of segments I increases, additional windowing with slower fall-off is introduced causing an increase in the out-of-band power of the clipped signal, and so to the spectral regrowth. In fact, the number of segments I determines the number of zero-departures and zero-arrivals in the clipped signal portion. These zero-departures/arrivals in the clipped signal portion represent the threshold crossings N_C in the input signal to the PD-HPA.

Therefore, it is deduced that the signal characteristics at the input of the PD-HPA that mainly contribute to spectral regrowth in relation to the PD-HPA clipping threshold are the variance of signal portion exceeding the threshold σ_c^2, the threshold crossing rate $R_C = N_C/L$, and the time durations of the crossing events τ_i's. Unfortunately, no convenient method of exact calculation of τ_i is available as yet [8, 13]. Therefore, in such an approach, the mean threshold crossing duration $\overline{\tau}$ is used as an indicator to the durations of crossing events.

4. Existing Nonlinearity Severity Measure

Several measures were adopted to quantify NLD in relation to the input signal to the HPA. PAR is the most commonly used measure of the potential nonlinearity due to HPAs, which when reduced decreases the dynamic range of the input signal to the HPA. In turn, the signal traverses a smaller range of the inherent nonlinearity of the HPA transfer function. Several techniques have been proposed to reduce

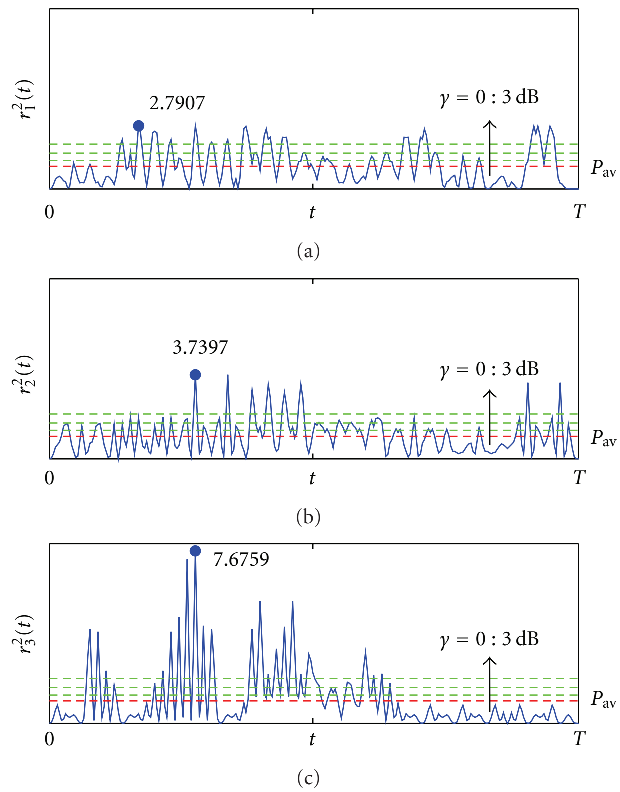

Figure 3: Instantaneous powers $r_1^2(t)$, $r_2^2(t)$, and $r_3^2(t)$ of representations R1, R2, and R3, respectively, at different IBOs γ.

the PAR, such as clipping [14], companding [15], selected mapping (SLM) [16], partial transmitted sequences [17], and Walsh code reassignment techniques [1, 18]. For a signal $s(t)$ of duration T, $E\{s(t)\} = 0$, the PAR ψ is defined as

$$\psi = \frac{\max_{0\le t\le T} |s(t)|^2}{E\left\{|s(t)|^2\right\}}. \tag{24}$$

Recently, other measures have been adopted such as the instantaneous power variance (IPV) [3, 4, 6] and the cubic metric (CM) [5, 6]. The motivation for the IPV measure is to reduce the envelope fluctuations [6]. The IPV $\sigma^2_{|s|^2}$ is defined normalized to remove the dependence on the average power as [4]

$$\sigma^2_{|s|^2} = \frac{\text{var}\left\{|s(t)|^2\right\}}{[\text{var}\{s(t)\}]^2} = \frac{E\left\{|s(t)|^4\right\}}{\left[E\left\{|s(t)|^2\right\}\right]^2}. \tag{25}$$

The CM measure was proposed with the motivation of reducing the third-order modulation product as it is the cause of the major distortion [5]. The CM is defined as

$$\text{CM} = \sqrt{E\left\{\left(|s_{\text{rms}}|^3\right)^2\right\}}, \tag{26}$$

where s_{rms} is the root mean square (rms) value of $s(t)$.

While the above-mentioned measures have their use and have led to remarkable improvements, none of them has

Table 1: Signal Characteristics of R1, R2, and R3.

	R1	R2	R3		
PAR (dB)	**4.46**	5.73	8.85		
IPV	0.61	**0.51**	1.51		
CM	0.36	0.36	**0.12**		
R_E	0.432	0.489	**0.337**	0	
	0.280	0.341	0.322	1	
	0.246	**0.164**	0.212	2	
	0.140	**0.083**	0.155	3	
σ_c^2	0.058	0.125	**0.048**	0	γ (dB)
	0.027	0.033	0.142	1	
	0.015	**0.015**	0.097	2	
	0.006	**0.004**	0.063	3	
BER	0.137	0.146	**0.129**	0	
	0.124	0.129	0.131	1	
	0.121	**0.115**	0.121	2	
	0.113	**0.109**	0.116	3	

a close relation with the system performance. In other words, no clear mathematical relation exists between these measures and the resulting different forms of NLD (BER degradation and spectral regrowth). Accordingly, their reduction does not always lead to optimum performance. An example to illustrate the above idea is presented, where the BER is considered as the performance merit. The reader is reminded that it was established in [7], as presented in Section 3.1, that the signal characteristics contributing to BER degradation caused by amplifier nonlinearity are the threshold exceeding rate R_E and the variance of the clipped signal portion σ_c^2.

Consider an example 16-user CDMA signal of duration T with Walsh codes of length $L = 64$ and filtered with an SRRC filter. Many representations of this signal have been generated. Three of them were selected in order to emphasize that the above-mentioned measures do not always lead to optimum performance. The three representations (R1, R2, and R3) of such a signal are generated with the same average power P_{av} using the SLM technique [16]. Figure 3 shows the instantaneous power of the three representations $r_1^2(t)$, $r_2^2(t)$, and $r_3^2(t)$. The PAR, IPV, and CM are calculated for each representation. Also R_E and σ_c^2 are measured for each representation at different values of IBO γ and tabulated in Table 1.

It is clear in Table 1 that, among the three representations, R1 has the minimal PAR, R2 has the minimal IPV, and R3 has the minimal CM. Looking to the calculated parameters in Table 1, it can be observed that a representation with a minimal of one of the considered measures might have higher values of R_E and σ_c^2 at certain IBO values. Hence, such a representation, according to the analysis in Section 3.1, will be more vulnerable to NLD leading to worst BER degradation. For instance, R1 has the lowest values of R_E and σ_c^2 only at IBO = 1 dB, while has higher values than those of R2 and R3 at other IBO values. Similarly, R2 has the lowest values of R_E and σ_c^2 at IBO = 3 dB and 4 dB, while has higher values than those of R1 and R3 at other IBO values. Also, R3 has the lowest values of R_E and σ_c^2 at IBO = 0 dB, while has higher values at other IBO values. Moreover, at SNR_{AWGN} of 5 dB and using the measured values of R_E and σ_c^2, the BER for all representations at the considered IBO levels are computed based on the BER in (16). It is evident, from the BERs in Table 1, that a representation with a minimal value of one of the nonlinearity measures of interest may achieve the best performance at certain IBO threshold values and fail at others. Therefore, it is concluded that the considered measures are not closely related to the system performance and do not always lead to the optimum performance. Also, an important conclusion should be clear here, which is the necessity to involve the IBO threshold level in the formulation of any nonlinearity measure.

It is worth mentioning another measure that is close to PAR is the peak-to-mean envelope power ratio (PMEPR), which is defined in [19] for Rayleigh-distributed envelopes as

$$\text{PMEPR} = \frac{X^2(\mathcal{P})}{2\sigma_x^2}, \tag{27}$$

where $X(\mathcal{P}) = \sqrt{-2\sigma_x^2 \log \mathcal{P}}$ is the envelope value that is exceeded with probability $\mathcal{P} = P(r > X) = \int_X^\infty f_r(r)dr = e^{-X^2/2\sigma_x^2}$, resulting in $\text{PMEPR} = -\log \mathcal{P}$.

Regarding the PAR (or PMEPR) issue particularly, it can be justified as follows. In the presence of a PD-HPA, the signal dynamic range is already determined by its threshold, after which the output signal is clipped (distorted). Accordingly, using the dynamic range in terms of peak power as a measure for NLD loses its importance, and in this case, it is better to sacrifice high peaks by letting them be clipped in favor of keeping larger portions of the signal in the linear region below the PD-HPA threshold.

5. Nonlinearity Severity Measure

Based on the above discussion, we propose an efficient measure to quantify the severity of NLD, as an alternative to the existing measures, namely, nonlinearity severity (NLS) measure.

We define the NLS measure in a manner with similarities to the threshold crossing intensity parameter of [20], but explicitly using the signal characteristics directly related to BER performance and spectral regrowth (σ_c^2, R_E, R_C, and $\overline{\tau}$).

For the sake of having a simplified measure, it is useful to use the interesting relation between R_C and $\overline{\tau}$, where their product gives R_E [13, 21]. Thus, it can be argued that the signal characteristics affecting the overall system performance, in relation to NLD, are limited to R_E and σ_c^2. Thus, the NLS measure is defined as

$$\text{NLS}(s(t); \gamma) = \frac{R_E(\gamma)\sigma_c^2(\gamma)}{\sigma_s^2}. \tag{28}$$

To emphasize the relation of the NLS measure and the signal characteristics contributing to BER degradation, recall the example drawn in Section 4 with adding four other

Table 2: Signal Characteristics of R1, R2, R3, R4, R5, R6, and R7.

	R1	R2	R3	R4	R5	R6	R7		
PAR (dB)	4.46	5.73	8.85	5.59	5.52	5.28	5.37		
IPV	0.61	0.51	1.51	0.56	0.59	0.55	0.51		
CM	0.36	0.36	0.12	0.36	0.34	0.29	0.32		
R_E	0.432	0.489	0.337	**0.323**	0.451	0.447	0.496	0	
	0.280	0.341	0.322	0.281	**0.285**	0.360	0.386	1	
	0.246	0.164	0.212	0.193	0.189	**0.170**	0.193	2	
	0.140	0.083	0.155	0.076	0.095	0.061	**0.057**	3	
σ_c^2	0.058	0.125	0.048	**0.050**	0.058	0.052	0.047	0	
	0.027	0. 033	0.142	0.034	**0.024**	0.028	0.035	1	γ (dB)
	0.015	0.015	0.097	0.022	0.018	**0.011**	0.014	2	
	0.006	0.004	0.063	0.010	0.008	0.006	**0.004**	3	
NLS (dB)	−15.98	−12.15	−17.90	**−17.92**	−15.85	−16.35	−16.30	0	
	−21.24	−19.43	−13.41	−20.39	**−21.59**	−19.89	−18.67	1	
	−24.23	−26.16	−16.87	−23.81	−24.64	**−27.51**	−25.83	2	
	−30.47	−35.07	−20.08	−31.18	−31.29	−34.55	**−36.52**	3	

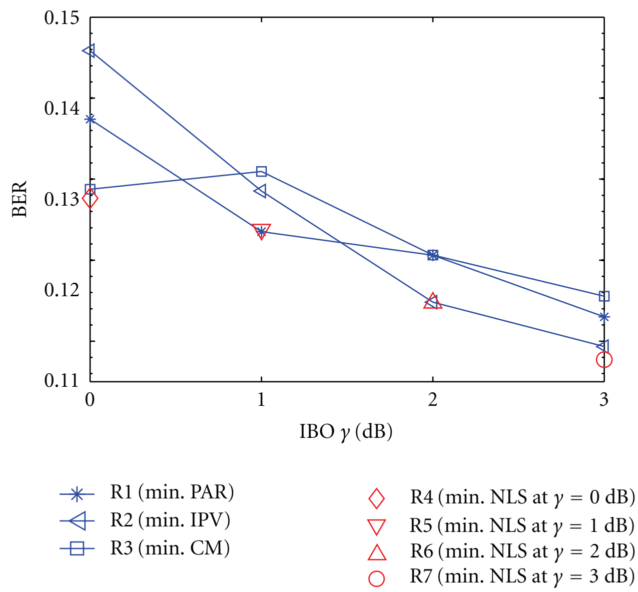

Figure 4: BER of (16) computed for R1–R7 versus IBO levels.

representations R4, R5, R6, and R7, which are selected such that they have a minimal NLS at IBO = 0, 1, 2, and 3 dB, respectively. The NLS measure is measured for all representations and shown along with the other parameters of interest in Table 2.

As can be seen in Table 2, for each of the IBO levels of interest, the values of R_E and σ_c^2 and measured for the representations with the minimum NLS are the minimal or very close to the minimal values of R_E and σ_c^2 and measured for the other representations. Also, the BER measured for all representations at all IBO levels is computed at SNR_{AWGN} of 5 dB and shown in Figure 4, where it is clear that the representations with minimal NLS adjusted to a particular IBO level lead to the best BER performance at that level.

It appears evident here is another advantage of the NLS measure, in addition of being directly linked to the BER performance and spectral regrowth, which is the correlation between the NLS measure and the IBO level. This means that we now have an effective measure for NLD commensurate with the IBO level required to work at according to design requirements or service regulations. Accordingly, the effects of NLD can be reduced by minimizing such a measure as will be shown in the next section.

6. Performance Assessment

Two performance merits are used in the assessment: BER and adjacent channel power ratio (ACPR) as a measure for spectral regrowth. The SLM technique is adopted as a platform for performance assessment. In SLM, several representations of the signal to be transmitted are generated, where there should be a selection criterion, upon which the best representation is selected for transmission.

Although any of the nonlinearity measures (PAR, IPV, and CM) described in Section 4 can be used as a selection criterion in SLM, PAR is the most commonly used and appears to be the state of affairs until now. This may be because of its simpler form and the numerous investigations and discussions conducted on it in the literature. Accordingly, in this paper, the performance of the NLS is assessed in comparison with PAR as selection criteria in SLM.

The concept behind the SLM technique is based on creating Q equivalent representations of the same signal $s(t)$ by rotating the phases of the data symbols such that $s(t), \in \{s^{(q)}(t)\}_{q=1}^{Q}$ [16]. Among the Q representations, the representation $\overline{m}$ that has the minimum PAR is selected for transmission. In our approach, the representation $\overline{m}$

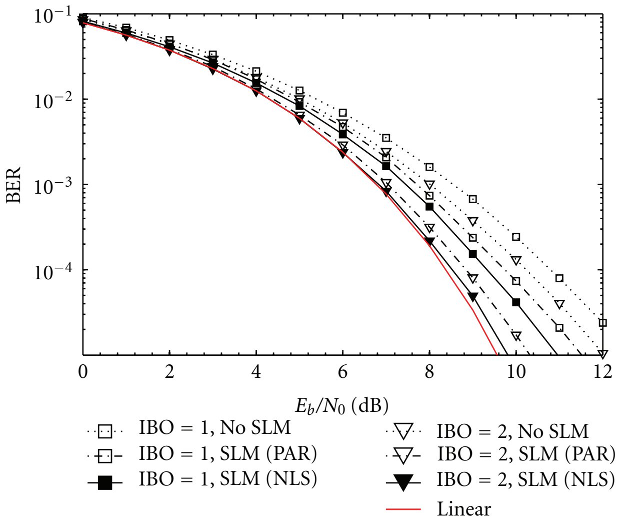

Figure 5: BER of 16-user CDMA signals in presence of PD-HPA.

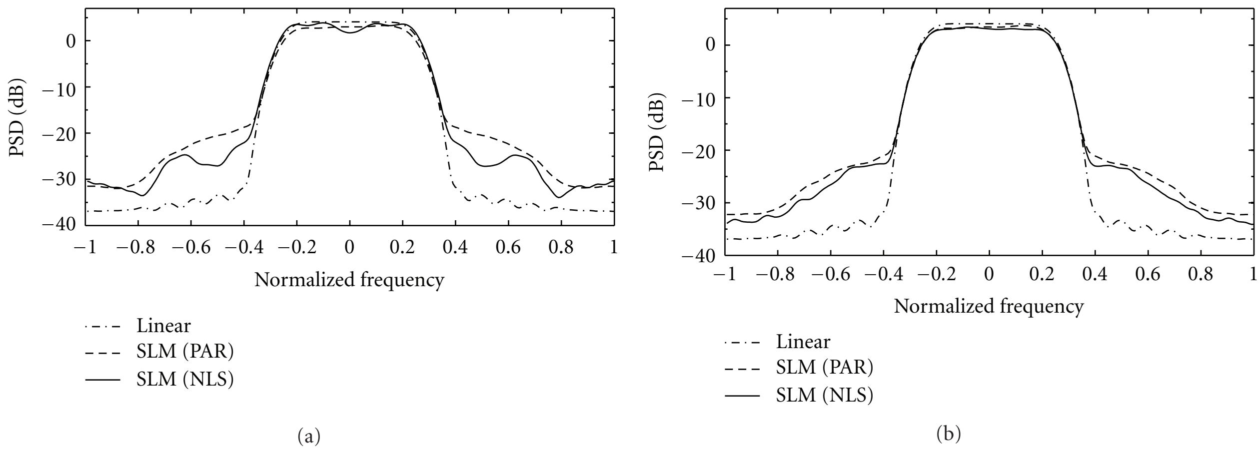

Figure 6: PSDs of 16-user CDMA signals in presence of PD-HPA at (a) IBO = 1 dB and (b) IBO = 2 dB.

that has the minimum NLS is selected for transmission as follows:

$$\overline{m} = \arg \min_{1 \leq q \leq Q} \text{NLS}^{(q)}(s(t); \gamma). \tag{29}$$

In this scenario, we have considered a CDMA system with Walsh orthogonal codes of length $L = 64$. An SRRC pulse shaping filter is used with roll-off factor of $\rho = 0.22$ and upsampling factor of 4 in order to obtain an adequate signal representation in a nonlinear environment. Three different representations for the CDMA signal are generated as follows: (1) with no SLM optimization, (2) with SLM using the minimum PAR as the selection criterion, and (3) with SLM using the minimum NLS adjusted to the IBO level of interest as the selection criterion.

The presented BER performance results represent the average BER of 100 frames of each CDMA signal representation of interest. Each frame consists in 10,000 random QPSK data symbols. The BER curves for 16-user CDMA signals in the presence of a PD-HPA at IBO of 1 dB and 2 dB are plotted in Figure 5. It is clear from the figure that using the minimum NLS measure, compared to the minimum PAR as selection criteria to select the signal to be transmitted, improves the BER performance. This was expected because the NLS measure is based on factors linked directly to the BER performance, R_E and σ_c^2, as we showed in (16).

To compute the ACPR, the PSD of each time domain signal representation of length $10L$ (Walsh code length) is computed. The PSDs are evaluated using the Welch estimation method with the following parameters: Hamming window, segment length of 32, and 50% overlap between segments.

The PSDs of the signal representations with minimum PAR and minimum NLS are plotted in Figure 6. The PSDs of the signal

representations with no SLM optimization are omitted from the plots to allow for clearer comparisons between the two representations we are interested in. However, the results of the computed ACPRs for all representations are tabulated in Table 3.

Table 3: ACPR for 16-OFDM in Presence of PD-HPA.

	ACPR (dB)	
IBO, γ (dB)	1	2
No SLM	−25.23	−26.82
SLM (PAR)	−26.18	−28.18
SLM (NLS)	**−27.42**	**−29.46**
Linear	−37.12	

It is clear from the PSDs in Figure 6 and the computed ACPRs that using the minimum NLS measure adjusted to the IBO level of interest, compared to the minimum PAR as selection criteria to select the signal to be transmitted, leads to less out-of-band

emissions. In turn, lower spectral regrowth is achieved.

It is worth mentioning that a representation selected based on the minimum NLS criterion may also have the minimum PAR. In this case, both criteria will lead to the same performance.

7. Conclusion

In this paper, it is shown that the existing measures for NLD are not correlated well with the overall system performance. We concluded that there are two reasons for such an uncorrelation: first, the absence of a clear direct relation between these measures and the system performance, second, the disinvolvement of the IBO level in the formulation of such measures. Hence, based on the established signal characteristics contributing to BER degradation and spectral regrowth, we introduced a new alternative measure, NLS, to characterize NLD effects on CDMA signals. When formulating the NLS measure, we were keen to avoid the above-mentioned drawbacks by relying on the signal characteristics contributing to BER degradation and spectral regrowth. Additionally, being a function in the IBO level gives the NLS measure a superior advantage as it can be adjusted to the IBO level required to work at according to design demands or service regulation.

Using such a measure, an efficient CDMA system is achieved through the provision of (1) a potential estimate of NLD effects on the transmitted signal and (2) the ability to minimize such effects as shown in Section 6, where the NLS measure showed an outperformance over PAR when used as a selection criterion in the SLM technique.

Finally, it seems that the NLS measure would be more complex than PAR. However, nothing is priceless. A little bit more complexity is the price paid for more improved efficiency.

References

[1] V. K. N. Lau, "On the analysis of peak-to-average ratio (PAR) for IS95 and CDMA2000 systems," *IEEE Transactions on Vehicular Technology*, vol. 49, no. 6, pp. 2174–2188, 2000.

[2] H. Ochiai and H. Imai, "On the distribution of the peak-to-average power ratio in OFDM signals," *IEEE Transactions on Communications*, vol. 49, no. 2, pp. 282–289, 2001.

[3] A. Behravan and T. Eriksson, "Some statistical properties of multicarrier signals and related measures," in *Proceedings of the 63rd IEEE Vehicular Technology Conference (VTC '06)*, pp. 1854–1858, July 2006.

[4] R. N. Braithwaite, "Using Walsh code selection to reduce the power variance of band-limited forward-link CDMA waveforms," *IEEE Journal on Selected Areas in Communications*, vol. 18, no. 11, pp. 2260–2269, 2000.

[5] H. Heng and Y. X. Yun, "Cubic metric and PAPR of OFDM-CPM signal," in *Proceedings of the 4th International Conference on Wireless Communications, Networking and Mobile Computing (WiCOM '08)*, pp. 1–3, October 2008.

[6] M. Deumal, A. Behravan, T. Eriksson, and J. L. Pijoan, "Evaluation of performance improvement capabilities of PAPR-reducing methods," *Wireless Personal Communications*, vol. 47, no. 1, pp. 137–147, 2008.

[7] T. Helaly, R. Dansereau, and M. El-Tanany, "Analysis of E performance in presence of nonlinear distortion due to PD-HPA in downlink DS-CDMA signals," *IEEE Communications Letters*, vol. 14, no. 4, pp. 273–275, 2010.

[8] T. Helaly, R. Dansereau, and M. El-Tanany, "Factors affecting spectral regrowth in DS-CDMA signals due to PD-HPA nonlinear distortion," in *Proceedings of the 72nd IEEE Vehicular Technology Conference (VTC '10)*, pp. 1–5, September 2010.

[9] R. Dinis and A. Palhau, "A class of signal-processing schemes for reducing the envelope fluctuations of CDMA signals," *IEEE Transactions on Communications*, vol. 53, no. 5, pp. 882–889, 2005.

[10] A. Conti, D. Dardari, and V. Tralli, "An analytical framework for CDMA systems with a nonlinear amplifier and AWGN," *IEEE Transactions on Communications*, vol. 50, no. 7, pp. 1110–1120, 2002.

[11] L. Rugini, P. Banelli, and S. Cacopardi, "Theoretical analysis and performance of the decorrelating detector for DS-CDMA signals in nonlinear channels," *IEEE Transactions on Wireless Communications*, vol. 3, no. 2, pp. 367–372, 2004.

[12] J. Proakis, *Digital Communications*, McGraw-Hill, New York, NY, USA, 4th edition, 2001.

[13] D. R. Morgan, "On level-crossing excursions of Gaussian low-pass random processes," *IEEE Transactions on Signal Processing*, vol. 55, no. 7, pp. 3623–3632, 2007.

[14] X. Li and L. J. Cimini Jr., "Effects of clipping and filtering on the performance of OFDM," in *Proceedings of the 47th IEEE Vehicular Technology Conference*, vol. 3, pp. 1634–1638, May 1997.

[15] T. Jiang, Y. Yang, and Y.-H. Song, "Exponential companding technique for PAPR reduction in OFDM systems," *IEEE Transactions on Broadcasting*, vol. 51, no. 2, pp. 244–248, 2005.

[16] R. W. Bäuml, R. F. H. Fischer, and J. B. Huber, "Reducing the peak-to-average power ratio of multicarrier modulation by selected mapping," *Electronics Letters*, vol. 32, no. 22, pp. 2056–2057, 1996.

[17] H.-G. Ryu, T. P. Hoa, K. M. Lee, S.-W. Kim, and J.-S. Park, "Improvement of power efficiency of HPA by the PARR reduction and predistortion," *IEEE Transactions on Consumer Electronics*, vol. 50, no. 1, pp. 119–124, 2004.

[18] A. G. Shanbhag and E. G. Tiedemann, "Peak-to-average reduction via optimal Walsh code allocation in third generation CDMA systems," in *Proceedings of the 6th IEEE International Symposium on Spread Spectrum Techniques and Applications (ISSSTA '00)*, vol. 2, pp. 560–564, September 2000.

[19] R. Dinis and A. Gusmão, "A class of nonlinear signal-processing schemes for bandwidth-efficient OFDM transmission with low envelope fluctuation," *IEEE Transactions on Communications*, vol. 52, no. 11, pp. 2009–2018, 2004.

[20] W.-Z. He and M.-S. Yuan, "Statistical property of threshold-crossing for zero-mean-valued, narrow-banded gaussian processes," *Applied Mathematics and Mechanics*, vol. 22, no. 6, pp. 701–710, 2001.

[21] J. E. Mazo, "Asymptotic distortion spectrum of clipped, DC-biased, Gaussian noise," *IEEE Transactions on Communications*, vol. 40, no. 8, pp. 1339–1344, 1992.